RESEARCH ARTICLE



Climatic controls on soil and saprock nitrogen distribution and persistence in the Sierra Nevada

Kimber C. Moreland^{1,2} Morgan E. Barnes^{3,2} Anthony O'Geen⁴ Nicholas Dove^{5,2} Stephen C. Hart² Asmeret Asefaw Berhe²

Correspondence

Kimber Moreland, Center for Accelerator Mass Spectrometry, Lawrence Livermore National Laboratory, Livermore, CA, USA. Email: moreland3@llnl.gov

This article has been edited by Marcus Schiedung.

Abstract

Background: Nitrogen (N) is an essential nutrient in soil that regulates plant growth, terrestrial sequestration of atmospheric carbon dioxide, and persistence of organic compounds. However, major knowledge gaps remain about how climate change may impact N accumulation and persistence, especially in deep soil and saprock (friable weakly weathered bedrock).

Aims: Our objective was to understand how climate impacts the accumulation of N in soil and saprock and how climate impacts soil N distribution, persistence, and mechanisms of N persistence.

Methods: We investigated N concentration in bulk soil and density fractions. We estimated N persistence along a bio-climatic sequence—sites range from a low-elevation oak savannah, mid-elevation pine-oak/mixed-conifer forest, to a high-elevation subalpine forest—in the southern Sierra Nevada in California. A combination of radiocarbon and elemental composition measurements along with a first-order kinetic model was used.

Results: The N concentration in the bulk soil and density fractions declined with depth, and there was a relatively greater mineral-associated heavy fraction (HF) N in deeper samples. The cooler/wetter mixed conifer site held 37% of profile N in saprock, which was greater than that of the entire soil profile at the drier/hotter oak savannah. The majority of N in soil, which was in the HF, was not influenced by climate proxies tested. However, both unprotected and occluded fractions of N were strongly influenced by climate. Soil N mean residence time (MRT) showed that drier/hotter climates have a shorter MRT, compared to mid-elevation sites with cooler/wetter climates.

Conclusions: The effect of climate on deep saprock N storage might be indirect, primarily through climatic influence on the thickness of saprock. Overall, our findings suggest the mineral-associated HF N pool will not be vulnerable to changes in climate and will continue to contribute to the persistent soil N pool. The amount of topsoil and subsoil unprotected and occluded N can be explained by gross primary productivity and mean annual precipitation indicating that changes in climate can influence N partitioning. N stored in deep soil and saprock may be less vulnerable to climate than N stored in

This is an open access article under the terms of the Creative Commons Attribution License, which permits use, distribution and reproduction in any medium, provided the original work is properly cited.

© 2022 The Authors. Journal of Plant Nutrition and Soil Science published by Wiley-VCH GmbH

¹Center for Accelerator Mass Spectrometry, Lawrence Livermore National Laboratory, Livermore, California, USA

²Department of Life and Environmental Sciences and Sierra Nevada Research Institute, University of California, Merced, CA, USA

³ Pacific Northwest National Lab, Richland, Washington, USA

⁴Department of Land, Air, and Water Resources, University of California, Davis, California, USA

⁵Biosciences Division, Oak Ridge National Laboratory, Oak Ridge, Tennessee, USA



drier/hotter climates with less deeply stored N. It is critical to dig deeper to understand terrestrial ecosystems' response to climate.

KEYWORDS

critical zone, deep soil nitrogen, nitrogen persistence, regolith, radiocarbon, ¹⁵N, density fractionation, weathered bedrock, saprock, saprolite

1 | INTRODUCTION

Nitrogen (N) is a plant essential nutrient that controls microbial functioning, plant growth, and the cycling of soil organic matter (SOM; Chapin et al., 2011; Houlton & Morford, 2015; LeBauer & Treseder, 2008). The majority of N in soils is found in the form of organic biomolecules, and its distribution parallels that of soil organic carbon (C; Berhe & Torn, 2017; Weil & Brady, 2016). Despite soils storing up to 50% of their total N (TN) below 0.3 m (to 1 m) globally (Batjes, 1996), our understanding of soil N dynamics in deep soil layers is extremely limited. The average sampling depth, since 2000, of the leading four soil journals is 0.23 m, suggesting that we do not fully understand both soil and saprock (the portion of the soil profile that retains structural parent rock fabric after having been weathered into a friable substrate in situ and has substantial porosity) N dynamics and how climate will impact them (Yost & Hartemink, 2020). This is concerning because the estimated global average soil thickness is 2 m with some soils extending down to 50 m, indicating that a massive portion of the soil system is missing (Shangguan et al., 2017). Recently, controls on the availability of soil N and how it is likely to affect C sequestration in a world with a changing climate has been a focus of a number of studies, especially for the topsoil (0-0.3 m; Craine et al., 2015; van Groenigen et al., 2015; Wieder et al., 2015). Consequently, there is now a pressing need to improve our understanding of soil and saprock N dynamics, including variables controlling subsoil (0.3-1 m) N pool distribution, persistence, and climate sensitivity.

Climate is one of the fundamental variables that control soil N dynamics, including TN input (rock weathering and N fixation) and N abundance (Houlton & Morford, 2015; Jenny, 1928). Changes in climate are expected to significantly influence overall soil nutrient cycling including N (Conant et al., 2011), with consequent effects on the structure, functioning, and diversity of terrestrial ecosystems (Sistla & Schimel, 2012). Among different climatic parameters, soil temperature and moisture stand out as key drivers that control soil N cycling (Bell et al., 2008). For example, lower soil moisture has been shown to lead to reduced N mineralization, increased nitrification, and increased N availability (Manzoni et al., 2012; Niboyet et al., 2011). Wang et al. (2016) found that reduced precipitation and warming amplified soil N turnover time in the top 0.16 m. Auyeung et al. (2015) demonstrated additional influence on N mineralization and nitrification with changes in moisture and temperature in the top 0.10 m. These prior studies illustrate climate does directly influence N persistence and dynamics.

Most soil warming N studies focus on the topsoil and have shown differing results in the response. For instance, a meta-analysis reported that with warming, topsoil net N mineralization rates increased by 46% with the greatest impacts observed in forested ecosystems (Rustad et al., 2001). Hart (2006) found that even small increases in mean annual temperature can greatly impact topsoil N cycling, soil-atmosphere trace gas exchange, and soil microbial communities. Larsen et al. (2011) and Rustad et al. (2001) found that warming increased net N mineralization, nitrification, and $N_2 O$ production rates. On the other hand, Niboyet et al. (2011) found little influence of warming on ammonia and nitrite oxidation (i.e., nitrification) in the top 0.05 m. In addition to this uncertainty, the lack of studies explicitly quantifying climate sensitivity of soil N below 0.5 m suggests there are major gaps in our ability to extrapolate these findings to include the whole soil and saprock N response.

C sequestration is driven by net primary productivity (plant photosynthesis), and N is essential for plant growth; therefore, if ecosystems are N-limited, it could constrain C sequestration (LeBauer & Treseder, 2008). There has been growing concern for nutrient N limitation and its ability to reduce ecosystem C sequestration because bioavailable forms of N are mobile and readily lost from ecosystems (Cleveland et al., 2013; Vitousek & Howarth, 1991). However, emerging studies have shown that rock N weathering plays important roles in ecosystem N and therefore C sequestration, especially in sedimentary parent materials (Houlton & Morford, 2015). A global analysis demonstrated that rock N inputs contributed roughly two to 11 times more to plant CO₂ capture than N deposition (Dass et al., 2021). Since climate impacts the rate of rock weathering (Dahlgren et al., 1997), and these aforementioned studies suggest that N rock weathering could greatly influence ecosystem N and therefore C sequestration, it becomes clear that it is important to understand the interactions between soil/saprock and N amount and persistence.

To further our understanding of how projected climate change can influence subsoil N accumulation and persistence, we conducted a complete accounting of the soil N pool including topsoil, subsoil, and saprock and derive mechanistic insights on the controls of whole soil N accumulation and persistence. The objective of this research was to determine how climate affects accumulation and persistence mechanisms of near-surface, compared to deep N. Specifically we asked two targeted questions:

- 1. Does climate affect the accumulation of N in soil and saprock?
- 2. How does climate influence soil N distribution, persistence, and the mechanisms responsible for N persistence?

18 | 100 years MORELAND ET AL.

TABLE 1 Sites at the Southern Sierra Critical Zone Observatory with the corresponding elevation (m asl), mean annual precipitation (MAP; mm year⁻¹), mean annual temperature (MAT; °C), evapotranspiration (ET; mm year⁻¹), gross primary productivity (GPP; g C m⁻² year⁻¹), and deep water percolation (DWP; mm year⁻¹)

Site	Elevation (m asl)	MAP (mm year ⁻¹)	MAT (C)	ET (mm year ⁻¹)	GPP (g C m ⁻² year ⁻¹)	DWP (mm year ⁻¹)
Oak savannah	400	502	16.6	395	480	212
Pine-oak	1160	860	13.8	749	1900	369
Mixed conifer	2020	994	9.2	564	1700	564
Subalpine	2700	1066	5.2	260	700	745

2 | MATERIALS AND METHODS

2.1 | Sites descriptions

The Southern Sierra Nevada Critical Zone Observatory (SSCZO) is a bio-climatic sequence in California. These sites are well suited to answer questions related to changes in climate because the bioclimatic sequence has soils developed under similar state factors of soil formation except climate, and consequently vegetation (Jenny, 1994). All the sites experience a Mediterranean climate, with cool, moist winters and warm, dry summers. The four study sites are on the western slope of the Southern Sierra Nevada: San Joaquin Experimental Range (oak savannah), Soaproot (pine-oak forest), Providence (mixed-conifer forest), and Shorthair (subalpine forest). As elevation increases, the mean annual air temperature decreases and the mean annual precipitation (MAP) increases (Table 1; Goulden et al., 2012). Actual evapotranspiration (ET) is highest in the mid-elevation sites and lower at the lowest elevation and highest elevation sites (Table 1; Goulden et al., 2012). The ET pattern has a positive correlation with the gross primary productivity (GPP). Deep-water percolation (DWP) was calculated as the difference between precipitation and ET (Goulden & Bales, 2014). The parent material for all sites is residuum granodiorite with igneous-felsic intrusive lithology except the lowest-elevation site, where the soil is derived from tonalite residuum (O'Geen et al., 2018). The parent material is thought to be of comparable age except the highest elevation site where bedrock was scoured by glaciers during the Last Glacial Maximum (Giger & Schmitt, 1983). Plant productivity and weathering are limited by low precipitation in the lowest-elevation oak savannah ecosystem, and by low temperature and historic glaciation in the high-elevation subalpine forest ecosystem causing changes in the thickness of the saprock (O'Geen et al., 2018). The boundary between soil and saprock was between 1.7 and 2 m at all sites, except the subalpine forest, where saprock did not exist. In all sites, except the subalpine, the thickness of saprock ranged from 2.25 to over 9 m, with the deepest Geoprobe core being over 10 m.

2.2 | Soil and regolith sampling

A total of 36 soil and saprock profiles were analyzed. At the oak savannah site (405 m), three Geoprobe (a hydraulic coring device, model DT22) cores and four pits excavated by a backhoe were sampled. At the pine-oak forest site (1160 m), five Geoprobe cores, five hand augers,

and five pits excavated by hand were sampled. Five Geoprobe cores, one hand auger, and four pits excavated by hand were sampled at the mixed-conifer forest site (2015 m). Only four hand-excavated pits were sampled at the subalpine forest site (2700 m) because of the relatively shallow depth of bedrock at this site. Soil pits were sampled by genetic horizons. Regolith is characterized as saprock that retains the relative positions of mineral grains of the parent bedrock. Saprock is a slightly weathered bedrock, where the original rock fabric is maintained but has become more porous and friable (Graham et al., 2010). The deepest sample of the saprock measured at each site was 2.70, 4.67, 10.67, and 1.15 m for the oak savannah, pine-oak forest, mixed-conifer forest, and subalpine forest sites, respectively. With hand augers, the depth of transition from soil to saprock was identified in the field by a change in color and consistency.

2.3 | General soil analysis

Particle size analysis on bulk pit samples (40 g air-dried and sieved [<2 mm]) was performed by the hydrometer (ASTM 152H) method. Bulk density of soil and saprock was measured using the core method (Dane & Topp, 2020). Three core samples were taken in each horizon from three soil profiles and averaged. They were oven-dried at 105°C until there was no weight change (24-48 h) and the >2 mm fraction and roots were removed. Samples were reported as the weight of the fine-earth fraction (<2 mm) divided by the volume of the fine-earth fraction. The volume percent of gravel in soil pits was estimated by dividing the weight of the coarse fraction by 2.65 mg m⁻³, dividing by the total volume of >2 mm plus <2 mm material, and multiplying by 100. Bulk density of lower saprock was measured by cutting an exact volume from the bottom 0.05 m of each core, which was sampled by the Geoprobe at 1-m depth intervals and oven-dried at 105°C. Soil pH was measured on air-dried and sieved soil (< 2 mm) in deionized water at a 1:2 (5 g:10 mL) soil-water suspension after 30 min, stirring every 10 min (Thomas., 1996). The pH meter used was an Accumet Basic, Model AB15, Fisher Scientific with an Ag/AgCl combination electrode.

2.4 | C and N analyses

Soil and saprock materials were air-dried, gently crushed, and sieved (2 mm mesh openings). Percentage of fine-earth (<2 mm) and coarse-earth fractions (>2 mm) were measured based on air-dry mass.

Fine-earth fractions were assumed to have no inorganic C due to acidic pH and testing for effervescence with 1M hydrochloric acid. Gravimetric water content was determined on air-dried subsamples by drying at 105° C until a constant mass. Total C and N concentration (%) of the fine-earth fraction was determined on samples ground to pass a 180- μ m sieve and analyzed by dry combustion (Costech Analytical ECS 4010 instrument, Costech Analytical Technologies, Inc., at the University of California, Merced and Davis).

TN pool (N_s , kg N m⁻²) was calculated from TN concentration (N_s , g kg⁻¹), thickness of the sample layers (d_c , cm) and bulk density (ρ_b , mg m⁻³), with correction for the weight percent of the coarse earth fraction (Equation 1).

$$N_{\rm s} = \Sigma N \times d_{\rm c} \times p_{\rm b} \times 100 \,. \tag{1}$$

2.5 Density fractionation

Density fractionation was used to separate the SOM into pools that are distinct in composition and to infer dominant mechanisms of SOM persistence (Lybrand et al., 2017; McFarlane et al., 2013; Swanston et al., 2002). The following fractions were separated: free light (debris outside aggregates, free light fraction [fLF]), occluded (light fraction inside aggregates, occluded light fraction [oLF]), and heavy fractions (HFs) organic matter (OM; bound to minerals, HF) separated using sodium polytungstate (SPT-O low C and N SPT, Geoliquids). Briefly, 30 g of airdried, sieved (<2 mm) soil was initially mixed with 1.7 g mL⁻¹ of SPT for 24 h; 1.7 g mL⁻¹ was chosen in order to compare across other studies done at these sites, and a density of 1.6-1.8 g mL⁻¹ is commonly used to exclude the most mineral and organo-mineral material from the light fractions while maximizing recovery of plant-like particulate OM (Young & Spycher, 1979). The fLF is first isolated by floating OM to the top as the supernatant where it is removed by aspiration and rinsed. To break up the aggregates and collect the oLF, the remaining sample was dispersed with ultrasonic energy at 2500 J mL $^{-1}$ (1500 J g $^{-1}$) with a Branson 450 Sonifier (Branson Ultrasonics) probe tip 0.05 m below the liquid surface and what floats to the top is collected as oLF and what remains at the bottom is HF. The dense particles, mineral HF, formed a pellet at the bottom after centrifuging. All three fractions were extensively rinsed with 0.01 M CaCl₂ to desorb the SPT and then deionized water and the fLF and oLF were filtered and rinsed using 0.8-µm filters (Lybrand et al., 2017). All samples recovered 85% or more N, compared to the bulk N after fractionation.

2.6 | Radiocarbon analysis

Radiocarbon analyses were conducted on soil samples after sealed-tube combustion of organic C to CO_2 (with CuO and Ag) that was then reduced onto Fe powder in the presence of H_2 (Vogel et al., 1984). Radiocarbon values were measured on the Van de Graaff FN accelerator mass spectrometer at the Center for Accelerator Mass Spectrometry at the Lawrence Livermore National Laboratory. OM

 δ^{13} C values were determined at the University of California, Merced, using a DELTA V Plus Isotope Ratio Mass Spectrometer (Thermo Fisher Scientific, Inc.). Radiocarbon isotopic values were corrected for mass-dependent fractionation with measured δ^{13} C values and were reported in Δ - notation corrected for 14 C decay since 1950 (Stuiver & Polach, 1977).

2.7 | Soil N accumulation model

To estimate the rate of N accumulation in bulk soil, the radiocarbon analysis and % TN were used in a first-order kinetic model of N accumulation (Berhe & Torn, 2017; Hilton et al., 2013; Jenny, 1994; Trumbore & Harden, 1997):

$$\frac{dN_{\text{pool}}}{dt} = I - k \times N_{\text{pool}},\tag{2}$$

where N_{pool} is the N pool in the bulk soil profile (kg m⁻²); I is the net N input to a soil pool from combined processes of atmospheric deposition, biological N fixation, and deposition of eroded topsoil (kg m⁻² year⁻¹); and k (year⁻¹) is the coefficient for first-order loss of N from soil through all particulate, dissolved and gaseous pathways. Equation (2) is solved subject to the initial conditions $N_{\text{pool}} = N_0$ at t = 0 at the start of N accumulation in the soil profile. Hence, assuming that $N_0 = 0$ at the beginning of soil development, Equation (2) is solved as

$$N_{\text{pool}}(t) = \frac{1}{k} [1 - \exp(-kt)].$$
 (3)

For each site, all four pits and the Geoprobe samples (after the deepest pit sample \approx 3 m Geoprobe samples were used to extend the profile to be drock to 5 m) were used in calculations of $N_{\rm pool}$. At the two mid-elevation sites, only soil samples taken to a maximum depth of 5 m were used in this calculation to avoid skewing the mean residence time (MRT) from the abundance of older radiocarbon ages from 5 to 10 m. This is because when calculating N_{pool} using Equation (3), the MRT of the mixed-conifer site were skewed by thousands of years due to the use of samples past 5 m that have radiocarbon ages up to 20,000 (Moreland et al., 2021) years causing worse model fit; therefore, we only used samples collected to a depth of 5 m. For example, when all of the data were included to 10 m, the sum of squares error was 17 as opposed to 5.1×10^{-1} when using the data to 5 m. We postulate that poor model fit is due to that radiocarbon values varied by more than 5 orders of magnitude below 5 m. The soil N_{pool} and the ¹⁴C radiocarbon ages from each pit and Geoprobe samples were used to derive cumulative N and estimated MRT of the N in each profile (Berhe et al., 2008; Berhe & Torn, 2017). For each soil profile, the N_{pool} in each horizon and then Geoprobe samples (thickness $\approx 0.5-0.7$ m) were summed at each depth increment to estimate the N accumulation between successive time stages. No tracer for estimating N MRT exists, so we assumed that N and C turned over at equivalent rates. This decision is based on our data and numerous other past studies that have shown that more than 95% of N in soils is organic and most organic N is covalently bonded to C-based SOM (Allison, 1973;

5222624, 2023, 1, Downloaded from https:

library.wiley.com/doi/10.1002/jpln.202200218 by University Of California,

Wiley Online Library on [31/07/2023]. See the Terms

on Wiley Online Library for rules of use; OA articles are governed by the applicable Creative Commons License



TABLE 2 Mean bulk density, clay concentration and pH (1:2 ratio of soil to deionized water) from each Master horizon and Cr horizon along the bio-climatic sequence

Site	Horizon	Average depths (m)	Bulk density (mg m ⁻³)	Clay (%)	pH (DI)
Oak savannah	А	0-0.28	1.46 ± 0.10	5.53 ± 0.81	5.38 ± 0.57
	В	0.28-1.08	1.63 ± 0.13	9.83 ± 5.06	5.70 ± 0.77
	С	1.08-1.30	1.64 ± 0.14	4.31 ± 0.94	6.14 ± 0.97
	Cr	1.30-1.86	1.67 ± 0.06	2.72 ± 2.52	5.81 ± 0.78
Pine-oak	Α	0-0.40	0.92 ± 0.33	5.40 ± 1.86	5.50 ± 0.38
	В	0.40-1.59	1.02 ± 0.46	6.84 ± 1.93	5.29 ± 0.56
	С	1.59-1.91	1.45 ± 0.18	10.97 ± 6.38	5.72 ± 0.85
	Cr	1.91-3.56	1.42 ± 0.00	8.50 ± 5.86	5.57 ± 0.65
Mixed conifer	Α	0-0.14	0.98 ± 0.22	3.26 ± 2.82	5.55 ± 0.08
	В	0.14-1.10	1.39 ± 0.13	6.08 ± 1.93	5.34 ± 0.27
	С	1.10-1.47	1.41 ± 0.09	6.91 ± 1.96	5.25 ± 0.45
	Cr	1.47-9.36	1.54 ± 0.13	5.44 ± 2.10	5.22 ± 0.18
Subalpine	Α	0-0.08	1.25 ± 0.10	3.23 ± 0.61	5.25 ± 0.30
	В	0.08-0.67	1.42 ± 0.14	4.27 ± 1.73	5.60 ± 0.29
	С	0.67-1.00	1.33 ± 0.09	3.66 ± 0.68	5.69 ± 0.25

Batjes, 1996; McGill & Cole, 1981). In addition, we found that the concentration of the bulk sample C and N were strongly correlated (R2 = 0.84, p = 0.049, n = 400), as has been shown previously (e.g., Berhe & Torn, 2017). For each pit, the N that accumulated between the successive time stages is summed into a total profile N accumulation, and the MRT is estimated from radiocarbon-based ages of each soil layer. The total profile N pool versus years of accumulation (t) was used to estimate I and k by fitting the data with Equation (3) to the data determined in Excel (MS Office 2011). Model fit was assessed by non-linear least squares. The accumulation starts from the bottom up because of the assumption that the deepest soil formed first and the OM associated with the soil layers on top formed later (Riebe et al., 2017).

2.8 Data analyses

Data are presented with mean ± standard error. ANOVA was performed on average clay % and bulk density to test if they significantly varied by site. Pairs of means at the different sites were compared using the Tukey--Kramer HSD test, and simple linear regression was used to assess the degree of covariance. For all statistical tests, an a priori significance level of p < 0.05 was used. All statistical tests were performed using R version 1.1.456. We used a random mixed effects model to assess the relationship between climate and soil N in fractions (mg N g⁻¹). We used individual climatic variables (GPP, ET, MAT, MAP, and DWP) as the fixed random effects and the independent variable of TN (mg N g⁻¹) of each fraction. The climatic variable values were taken from Goulden and Bales (2014), and deep water percolation is the difference between precipitation and ET. R² and p-values were calculated for each fraction within topsoil (< 0.3 m) or subsoil (> 0.3 m).

3 RESULTS

3.1 | Physical and chemical characterization of

Across the bio-climatic sequence, bulk density generally increased with depth for all sites and ranged from 0.92 mg m⁻³ in the A horizon to 1.67 mg/m³ in the Cr horizon (Table 2). The soils were generally coarsely textured with clay below 1%. Clay concentration increased from the A to B horizons on average by 1.6% across all sites. At the highest and lowest elevation sites, clay concentration decreased from the B to C horizon on average by 2.2%. The mid-elevation soils both increased in clay concentration from the B to C horizons. Soils across the bioclimatic sequence were strongly to moderately acidic, ranging from 5.2 and 6.1. There was no clear or consistent trend in pH change with depth for all sites (Table 2).

3.2 | Total N pool in soil and saprock

In all sites, soil contains more TN than the saprock with the soil TN pool accounting for 63% to 100% of the total soil profile N (Figure 1). Saprock accounted for a large proportion of the TN pool at midelevation sites (Figure 1). In soil, TN pool increased with elevation to a maximum of 0.75 kg N m⁻² at the mixed-conifer forest (2015 m) but decreased to 0.25 kg N m⁻² at the subalpine forest (2700 m; Figure 1). Soil TN content increased (relative to saprock) at the subalpine forest (2700 m) because this site did not have deep saprock (Figure 1). The N proportion in saprock went from 4% in the oak savannah to 23% in the pine-oak and then to 37% in the mixed-conifer forest (Figure 1). The

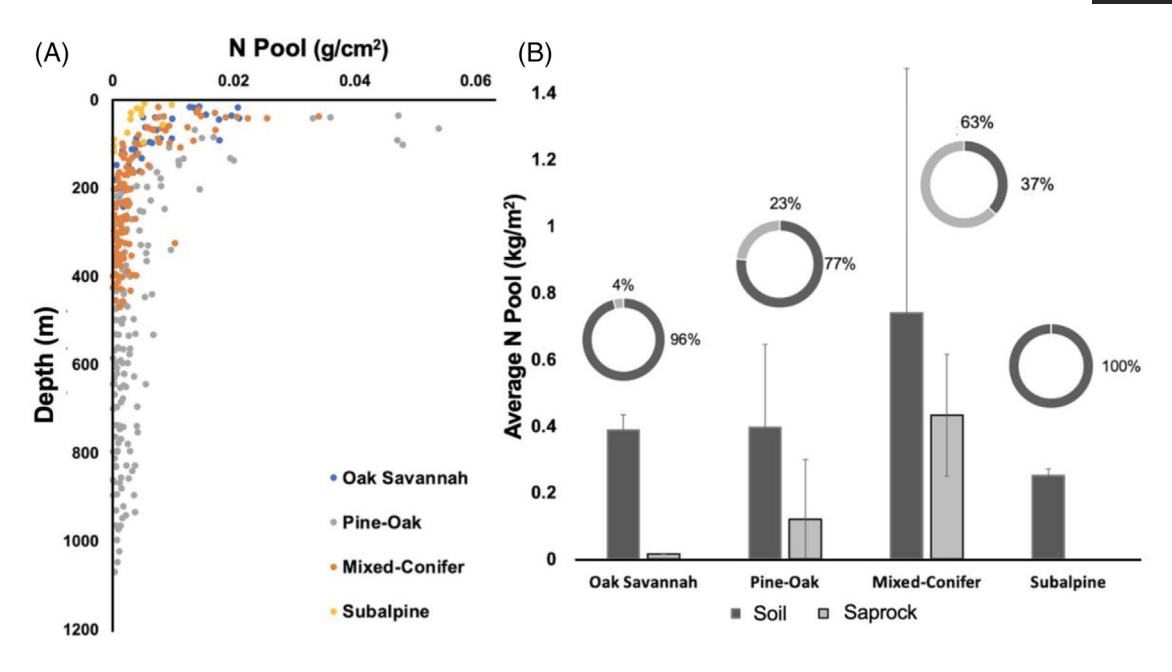


FIGURE 1 (A) Depth profiles across the bio-climatic sequence of nitrogen (N) pool (g cm $^{-2}$, n = 77). (B) Partitioning of N in soil and saprock across the bioclimatic gradient using Geoprobe-derived samples. Bar charts represent the total N (TN) pool (error bars represent standard deviations, n = 48) in soil and saprock. Pie charts represent the proportion of N pool of soil and saprock among the four study sites: oak savannah, pine-oak, mixed-conifer forest, and subalpine forest. Standard deviation is represented as the error bars.

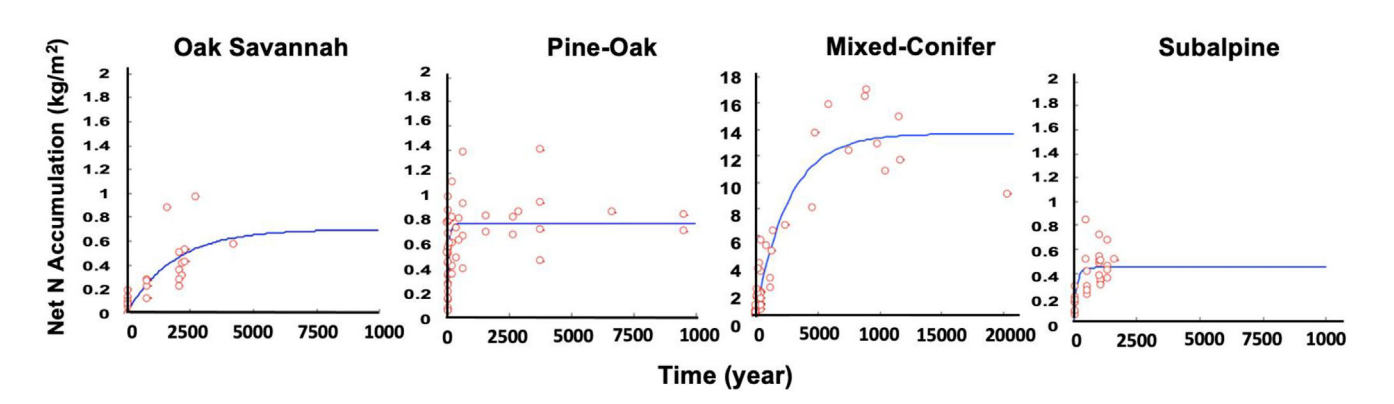


FIGURE 2 Modeled (blue line) and measured (red circles) net accumulation of soil and saprock N over time for all four sites of the Southern Sierra Critical Zone bio-climatic sequence. Samples include soil pit and Geoprobe-collected soils down to a 5-m depth. Years of accumulation were calibrated with radiocarbon ages of bulk samples taken from the soil pits and Geoprobe samples. Note: scales on both axes for the mixed-conifer site are greater than for the other sites.

saprock of some sites stored more N than the soil systems alone, for example, the oak savannah (405 m) stored 0.387 kg N m $^{-2}$ in soil, compared to the mixed-conifer forest saprock, which stored 0.432 kg N m $^{-2}$ (Figure 1).

3.3 Net N accumulation over time along the bio-climatic sequence

The rate of N accumulation varied considerably between sites based on the first-order model. During the early years of model simulation, the

rate of N accumulation was highest at the pine-oak and subalpine sites and occurred within a few hundred years (Figure 2). The oak savannah site reached a steady state right before 5000 years, the pine-oak site reached a steady-state N around 500 years, the mixed-conifer reached a steady-state N between 7500 and 10000 years, and the subalpine site reached a steady-state N in 500 years.

Results from our model showed that down to 5 m, the MRT of N increased with elevation from 64 years for the oak savannah to a maximum of 652 years for the mixed conifer and then decreased to 117 years for the subalpine site (Table 3). The modeled rate of N input in the mixed-conifer site was around 10 times slower than the oak savannah



TABLE 3 Mean TN pool (*Npool*) of soil and saprock and modeled values of whole soil profile-integrated net input of N to the soil N pool (I_N), modeled coefficient for first-order N loss from for the soil profile (k), and modeled mean residence time of N (MRT_N) in soil profiles at each site to 5 m

Site	$ \begin{array}{ccc} \textit{Npool} & & & I_{N} \\ \textit{(kg m}^{-2}) & & \textit{(kg m}^{-2} \textit{year}^{-1}) \end{array} $		k (year ⁻¹)	MRT _N (year ⁻¹)	Sum of squares of errors	
Oak savannah	0.5	6.4×10^{-03}	1.5×10^{-02}	64	1.3 × 10 ⁻⁰³	
Pine-oak	0.9	1.1×10^{-02}	1.4×10^{-02}	70	7.0×10^{-04}	
Mixed conifer	4.7	7.5×10^{-03}	6.9×10^{-04}	652	5.1×10^{-01}	
Subalpine	0.6	3.8×10^{-03}	8.5×10^{-03}	117	1.0×10^{-02}	

and pine-oak sites. The general trend suggested that drier and hotter climates (low elevation) have faster N MRT than cooler and wetter climates (Table 3).

3.4 N partitioning across fractions in topsoil versus subsoil

All density fractions decreased in N concentration from the topsoil (0-0.3 m) to the subsoil (0.30-1 m). N concentrations in both fLF and oLF decreased drastically (by an average rate of 0.5%) from 0 to 0.25 m and stayed relatively consistent below that depth. Comparatively, the N concentration in the HF decreased more than any other soil fraction with depth from 0 to 0.5 m (Figure 3A,F,K). However, the N concentration in each fraction decreases substantially with depth for both the fLF and oLF. There is more N in the topsoil fLF, compared to the topsoil oLF. The proportion of TN in the fLF and oLF decreased with depth, while the proportion of N in the HF generally increased with depth (Figure 3B,G,I). Radiocarbon concentrations (Δ^{14} C) were depleted (older) with depth for all fractions with the most depleted samples in the oLF and HF pools (Figure 3C,H,M). The stable N isotopic composition of δ^{15} N in the light fraction across the depth profiles at all sites mirror each other, where the δ^{15} N in all fractions becomes isotopically heavier from the A to B horizon but isotopically lighter from the B to C horizon (Figure 3E,J,O).

Figure 4 illustrates the average proportion of N in each fraction in the topsoil (0–0.3 m), subsoil (0.3–1 m), and below 1 m for each site. The proportion of fLF N is highest in the topsoil and declined with depth at all sites. In general, as elevation increased, the proportion of fLF N increased. The proportion of oLF N is also highest in the topsoil and declined with depth at all sites. The proportion of N in the HF fraction accounts for the largest proportion (over 50%) of N across all sites and depths (Figure 4). The highest proportion of N in the oLF and the largest difference, between the topsoil and subsoil, was also found in the midelevation sites. With depth, N in the fLF and oLF decreased in every site. As elevation increased, there was a greater proportion of N in the fLF and oLF.

Table 4 presents the results from a mixed-effect model for N distribution in the different fractions with elevation and the five climate variables. This provided insight into the relative contribution of climate in explaining the variability of N partitioning between topsoil, com-

pared to subsoil layers within the fractions. Considering topsoil fLF N (mg N g $^{-1}$), GPP explained 65% of the variation, MAP explained 66% of the variation, DWP explained 68% of the variation, and MAT and ET were not statistically significant. In the N (mg N g $^{-1}$) of the topsoil oLF, GPP explained 57% of the variation, MAP explained 66% of the variation, ET explained 28% of the variation, and MAT and DWP were not statistically significant. In the N (mg N g $^{-1}$) of the subsoil fLF DWP explained 26% of the variation, MAP explained 25% of the variation, and GPP, MAT, and ET were not statistically significant. In the subsoil oLF N (mg N g $^{-1}$), GPP explained 53% of the variation, MAP explained 54% of the variation, and GPP, MAT, and ET were not statistically significant. The HF did not significantly correlate to any of the climate proxies in the topsoil and subsoil (Table 4).

4 DISCUSSION

4.1 | Allocation of N in soil and saprock across the bioclimatic gradient

We demonstrated that climate indirectly impacts the TN pool in saprock through its influence on the thickness of saprock. This is evident in that sites that have a favorable climate help to create a thick saprock layer and consequently have larger TN pools (soil + saprock), compared to the other sites with little to no saprock. Over time, the parent material is weathered as a function of the five state factors of soil formation: climate, biota, parent material properties, relief, and time that regulate the input of material and efflux of byproducts, via a combination of abiotic and biotic weathering processes (Pope, 1995). The mid-elevation sites in the SSCZO extend down from 5 to 10 m depths, illustrating that the conditions are optimal for extensive loosening of the bedrock. Such conditions include increased volume of voids by activity of plants, animals, or physical processes and by removal of material by leaching (Buol et al., 1980; Moreland et al., 2021). Our results show that in the SSCZO bio-climatic sequence, the soil TN pool was highest at the mid-elevation sites (pine-oak and mixed-conifer forest) where climate optimizes GPP (Figure 1; Goulden & Bales, 2014; Kelly & Goulden, 2016). Our findings are consistent with previous studies using a bio-climatic sequence to show that soil development and weathering rates are maximized at the rain-snow transition with mesic temperatures and relatively high precipitation,

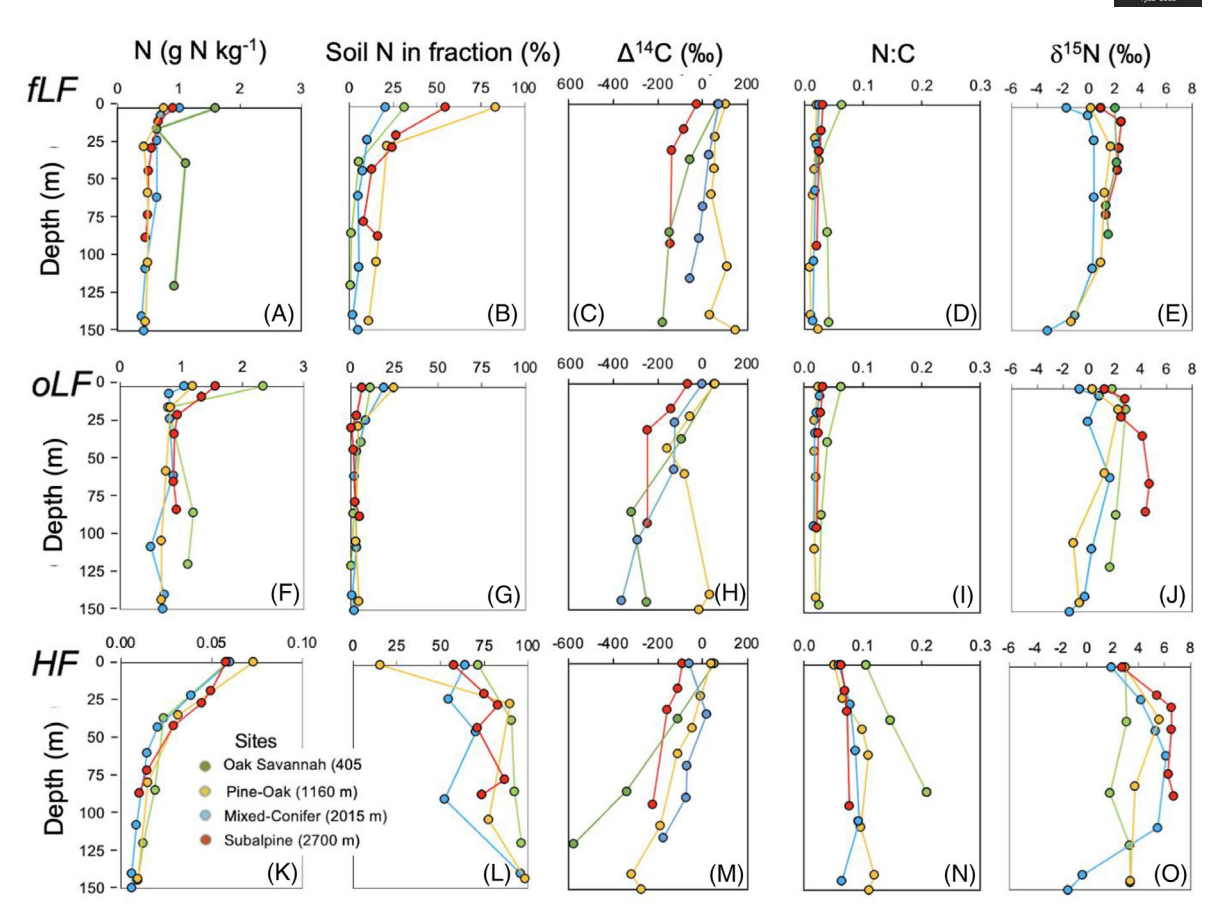


FIGURE 3 Mean N concentration (g N kg⁻¹), proportion of soil TN in each density fraction normalized to 100%, radiocarbon value Δ^{14} C (‰), weight ratio of nitrogen to carbon (N:C), and the δ^{15} N (‰) in free light fraction (fLF, A–E), occluded light fraction (oLF, F–J) and the heavy fraction (HF, K–O). n=3 for each point in every fraction, except some of the deepest samples were n=1. *Note that the heavy fraction N (HF N) concentration panel (K) has a different X-axis scale than the fLF and oLF (panels A and F, respectively).

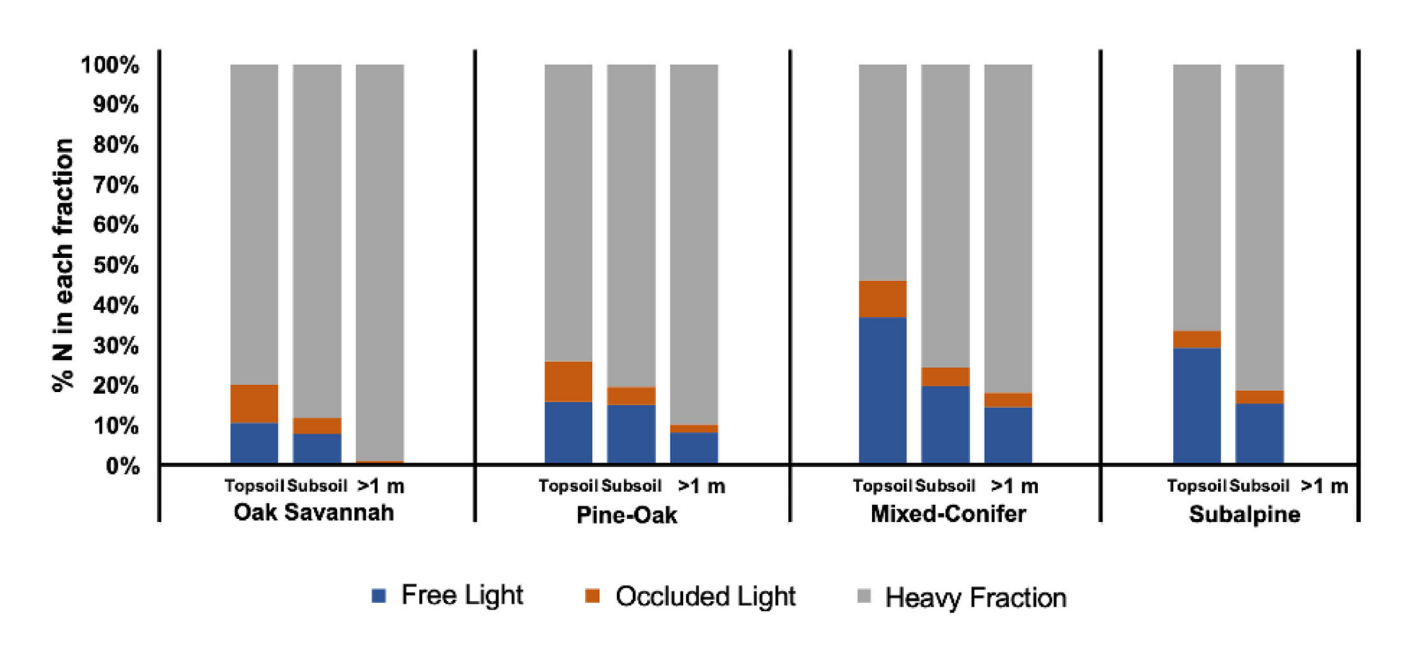


FIGURE 4 Mean proportion of N in each fraction in the topsoil (0-0.3 m), subsoil (0.3-1 m), and regolith below 1 m for each site. Means were normalized to 100% to account for any N loss during fractionation. Note that regoliths were <1 m deep at the subalpine forest site so there are no bars shown for >1 m.

24 | 100 years MORELAND ET AL.

TABLE 4 Mixed effect model results between N concentration in soil density fractions (g N kg $^{-1}$) and climate variables and proxies with conditional R-squared (R^2 C, includes random and mixed effects) and p-value (p < 0.05, p). Sample size (n) was 25 for topsoil and 38 for subsoil. Topsoil was grouped by A horizons equivalent to 0.3 m and subsoil was classified as the B and BC horizons going down to 1.5 m

Fraction		GPP		MAT		MAP		DWP		ET	
		R ² C	p-value								
Topsoil	fLF	0.654	<0.010*	0.681	0.051	0.662	<0.010*	0.682	0.042*	0.680	0.171
Subsoil	fLF	0.261	0.146	0.263	0.054	0.251	<0.010*	0.261	0.041*	0.252	0.701
Topsoil	oLF	0.574	<0.010*	0.332	0.141	0.663	<0.001*	0.493	0.053	0.283	<0.010*
Subsoil	oLF	0.528	0.010*	0.561	0.072	0.542	<0.010*	0.561	0.051	0.554	0.191
Topsoil	HF	0.136	0.065	0.001	0.873	0.221	0.173	< 0.010	0.963	0.141	0.065
Subsoil	HF	0.242	0.579	0.221	0.241	0.018	0.512	0.221	0.232	0.232	0.980

Abbreviation: fLF, free light fraction; HF, heavy fraction; oLF, occluded light fraction.

such as the mid-elevation pine-oak forest and mixed-conifer forests we studied (Dahlgren et al., 1997; Egli et al., 2003; Jenny, 1980; Rasmussen et al., 2007). Given that TN concentrations were relatively low in saprock, the main factor influencing the magnitude of N pools was thickness, and the systematic trends in thickness are controlled by climate. This low concentration of N in saprock mirrors the trends seen in the relative concentrations of organic C in soil, compared to saprock in the same study sites, where saprock C represents up to 30% of the total profile C pool (Moreland et al., 2021; Yang et al., 2022), compared to the 37% profile N being accounted for by saprock in this study. Recent studies are highlighting that, in addition to biological fixation of atmospheric N₂, the weathering of parent material can contribute to soil N pools and availability (Houlton & Morford, 2015). Houlton et al. (2018) found that more than 38% of the ecosystem N budget came from bedrock sources in temperate forest ecosystems. This indicates that saprock N sources have the potential to influence both nutrient cycling, C storage/sequestration, and vulnerability to changes in climate.

Subsoil and saprock N could originate from a combination of sources including dissolved OM, particulate OM, above- and below-ground vegetation, bioturbation, and geogenic N. As OM is mineralized, some of the mineralized N becomes mobile via dissolved and particulate OM leaching into the saprock (Klotzbücher et al., 2013). Kaiser and Guggenberger (2000) suggest that translocation of dissolved OM is one of the dominant mechanisms that moves OM deeper into soils and saprock. Dissolved N enters the mineral soil through root exudates, leaching of soluble plant litter, and atmospheric N deposition and has also been found to have a greater microbial signature in saprock (see Section 4.3 for further discussion on microbial processing; Gabor et al., 2014; Knicker, 2011; Sleutel et al., 2009). Sleutel et al. (2009) observed that a coniferous forest had up to 20% of dissolved N fluxes enter the mineral soil from the forest floor. Leaf litter, root litter, and root exudates are important sources of dissolved N that are translocated throughout the mineral soil. In some cases, root litter and exudates can contribute large amounts of N, compared to leaf litter N (Sleutel et al., 2009; Uselman et al., 2012). Once the N is in the mineral soil, it may cycle between roots, microbial biomass, adsorption and desorption from minerals, dissolution, and precipitation (Knicker, 2011). Because deeper soils and saprock have a larger volume of reactive surface, compared to the topsoil, percolating dissolved N could be one of the main sources of deep N.

Besides the contribution of dissolved and particulate N, N deeper in the regolith can be coming from bioturbation or geogenic sources. Bioturbation is when animals such as earthworms, termites, arthropods, fungi, and plant roots physically move soils and mix them. Bioturbation is also often cited as a major process influencing the vertical distribution of soil OM (Amundson et al. 2007; Tonneijck & Jongmans 2008). Biturbation, especially from animals, is likely to impact just the subsoil and not the saprock.

Another mechanism of deep N is related to the emplacement of geologic N through primary weathering and soil formation on parent rock containing N (Houlton & Morford, 2015). The contribution of geogenic N to total soil N may vary based on the mineralogy and geologic history of the parent material with N in higher concentrations in sedimentary rocks, compared to more trace amounts in igneous parent materials (Holloway & Dahlgren, 2002). Granite rocks have been found to contain N with low concentrations varying from 1 to 243 N mg kg $^{-1}$ (Holloway & Dahlgren, 2002). Stevenson (1962) suggests that the N in igneous rocks is the ammonium contained within potassium-bearing primary minerals such as mica and feldspar. X-ray diffraction analysis at these sites shows that the granitic parent materials consist of kaolinite, gibbsite, mica, vermiculite, smectite, and feldspars suggesting that some of the N in saprock could be rock derived, especially the mica and feldspar (Tian et al., 2019).

4.2 Differential rates of accumulation and MRT of N along the bio-climatic sequence

Maintaining SOM pools requires a balance between plant primary productivity and decomposition, both of which are affected by climate (i.e., temperature and moisture; F. A. Dijkstra & Morgan 2012). Vegetation drives maximum SOM input to the soil and varies across climatic regimes, primarily with moisture gradients (Jobbágy & Jackson, 2000). Results from our N accumulation model in the soil profiles illustrate that the rate of soil N accumulation and profile-averaged MRT of N is distinctly different in all the sites. The general steady-state trend

indicates that a drier and warmer climate (low elevation) will have a shorter MRT, and climates that are cooler and wetter will have longer N residence times until temperatures become cool enough to limit primary production, such as in the subalpine site (Table 3). Since the mid-elevation sites have a climate that is not too hot, dry, or cold, the above- and below-ground biomass (input) is higher, reducing N limitation and possibly explaining why there is a longer N residence time. The fLF and oLF TN amounts are higher in these mid-elevations, also suggesting more available N. Previous work at a similar mixed-conifer site as used in this study, estimated that the MRT of N of the forest floor was 7 years and the mineral soil (mostly A horizon) below that had an MRT of 34 years (Hart & Firestone, 1991). The authors suggested that this is due to increased microbial immobilization of N and a greater proportion of the total organic N mineralization in the O horizon, compared to below it (Hart & Firestone, 1991). This suggests that N is incorporated into the mineral soil system, and a larger proportion of the N persists in the mineral soil as opposed to the faster cycling organic (O) horizon. These results indicate that climate influences N MRT throughout the soil profile.

4.3 | Climatic influence on the distribution of N in soil fractions

Overall, our results suggest that climate does influence the distribution of N and mechanisms of N persistence. Results from the density fractionation show that most N throughout the profiles we studied is in the HF (Figure 4). HF N accounts for over 50% or more of TN. In the >1 m samples in the oak savannah, HF N accounts for over 95% of TN. This pattern is consistent with the density fractionation data from grassland sites in Northern California reported by Berhe and Torn (2017) where 90% of N was in the HF pool with parent material types that ranged in extent of crystallinity, indicating that even crystalline parent materials form HF mineral-associated N. The majority of soil organic N (SON) tends to be in the form of amides and amidecontaining compounds such as proteins, which are more likely to be charged molecules, increasing their affinity for mineral attachment (von Lützow et al., 2006). N-containing compounds can adsorb directly onto mineral surfaces reducing further translocation and vulnerability to oxidative attack by blocking enzyme attachment (Kögel-Knabner et al., 2008). Iron oxides and aluminum silicates may also play an important role in N retention, especially in deep soils because iron and aluminum mineral concentration generally increase with depth (Kaiser & Zech, 2000). OM associated with the mineral portion of soil is typically more persistent, compared to OM that is not sorbed or physically protected (von Lützow et al., 2006). Most of the N in all of the sites are in the HF pool, suggesting that this pool contributes substantially to the persistence of ecosystem N.

Mineral-associated—within aggregates and attached to primary and secondary minerals—OM is typically associated with slower MRT, recycled materials, and persistence (Schrumpf & Kaiser, 2015). Although our study did not identify the exact source of the N, however, a likely source for the HF N is microbial-derived dissolved organic N.

As the HF N increased with depth, the ratio of microbial-derived OM compounds, compared to the plant-derived compounds, increase, indicating a pattern of both microbially processed and newer material deposited deeper into the profile (Gabor et al., 2014; Moreland et al., 2021). Microbial-derived OM is likely to sorb onto soil minerals suggesting that some of the HF N may be microbially derived (Mikutta et al., 2019). The δ^{15} N of the HF is more enriched, compared to the fLF and oLF for all of the sites, except the oak savannah site, indicating that some of the HF pool could be microbially derived (Figure 3E,J,O; P. Dijkstra et al., 2006). However, granite δ^{15} N is reported to be between 1% and 10%, indicating that the HF δ^{15} N could also be representative of the parent rock and may not all be due to microbial processing (Holloway & Dahlgren 2002). Since the HF N pool increases with depth, this suggests that the subsoil N may be more persistent, compared to the topsoil, which is consistent with deep soil organic C at these sites (von Lützow et al., 2006; Moreland et al., 2021; Yang et al., 2022). HF N may be a large, overlooked persistent pool of N.

Soil OM found in the light fractions, which is fresher plant debris, typically cycles faster, compared to HF OM, and radiocarbon values are typically more depleted (get older) from fLF to oLF to HF (Schrumpf & Kaiser, 2015). We found important trends in the relative proportion of the light fractions (fLF and oLF) between sites that vary with climate, indicating that the accumulation of most N in the fLF and oLF is sensitive to changes in climate. As elevation increases, we observed a greater proportion of the soil TN contained within the fLF and oLF, mimicking C trends at these sites (Moreland et al., 2021; Rasmussen et al., 2005; Yang et al., 2022). This is due, in part, to the higher GPP at the higher elevation sites where there are greater inputs of N from aboveground plant and root sources (Goulden et al., 2012; Yang et al., 2022). Furthermore, the mixed effect model results indicate that variability in the topsoil and subsoil fLF and oLF can be explained most by GPP, MAP, and DWP. This also suggests that the higher elevation sites have more TN in the fLF and oLF because of higher GPP resulting in greater N cycling as GPP increases. However, because climate variables are highly correlated, it is difficult to discern which climate proxy is the driving force of these relationships. Follett et al. (2012) also found that soil organic N pools in the US Great Plains were strongly negatively related to MAT and positively related to MAP:PET, suggesting that soil N pools are vulnerable to increased temperature and decreasing water availability. Our study raises questions about the response of subsoil N to changes in climate and suggests that the subsoil fLF and oLF N may be more vulnerable than HF N.

Subsoil OM concentration decreases with depth and typically has a longer MRT, compared to topsoil (Jobbágy & Jackson 2000; Moreland et al., 2021; Yang et al., 2022). Lower concentrations of OM, lower microbial abundance, and increased persistence of OM due to burial, aggregation, and organo-mineral associations decrease the rate of subsoil OM decomposition (Chabbi et al., 2009; Rumpel & Kögel-Knabner, 2011; Schrumpf et al., 2013). Our results suggest that climatic controls appear higher for the surface than subsoil N. Trends in the models (lower R^2 in subsoil) suggest that less variability in the subsoil fLF, oLF, and HF can be explained by climate, indicating more persistent N in the subsoil that is less vulnerable to changes in climate, compared to

MORELAND ET AL.



topsoil fractions (Table 4). This interpretation is consistent with the finding that radiocarbon in the bulk soil and density fractions is more depleted (older) with depth (Moreland et al., 2021).

Even though subsoil OM is more persistent, compared to the topsoil, some studies have suggested that subsoil OM, and especially C, may be vulnerable to mineralization due to climate change (Hicks-Pries et al., 2017; Moreland et al., 2021; Yang et al., 2022). We observed increases in N:C ratios in soil with depth in the mineral-associated fraction and soils with more depleted (older) ¹⁴C in deep layers, suggesting more effective retention of N, compared to C, especially in the subsoil (Berhe & Torn, 2017). Previous studies suggested that bulk soil N:C trends with depth—if combined with increasing DON concentration (not measured in this study)—could indicate enrichment of more microbial-derived N in deeper soil layers (Kaiser & Kalbitz, 2012; Ros et al., 2009). This concept is also supported by the Fourier-transformed infrared spectroscopy and subsoil enrichment of d15N of the HF that suggested more microbially processed OM, compared to the fLF and oLF (Moreland, 2020; Figure 3E,J,O). Overall, these results suggest that the more labile topsoil N in the fLF and oLF may be vulnerable to changes in climate, whereas the topsoil HF and all the fractions in the subsoil may be less vulnerable to changes in climate and therefore could persist longer.

5 | CONCLUSION

Climate exerts both a direct and indirect control on soil N accumulation and persistence. Our bulk soil and saprock results evaluating the entire profile N from topsoil to bedrock suggest that the effect of climate on deep saprock N storage might be primarily through its effect on thickness, not necessarily the concentration of N in the regolith. The density fractionation results suggest that the mineral-associated oLF and HF pool contributes substantially to the persistence of N, especially in the subsoil, and is indirectly influenced by climate via weathering. N that becomes associated with minerals may be the pool where most of the accumulation and retention of soil N takes place, especially in deep soils. The modeled rate of N MRT and input indicated that a drier and warmer climate (low elevation) has a shorter MRT, and climates that are cooler and wetter have longer N residence times in soil.

The findings of our study highlight the important role of saprock in storing soil N and the interactions of different pools of soil N with climate. The critical zone science perspective used in our study allowed for an improved conceptualization of controls over N cycling and long-term ecosystem interactions between plants, soils, and saprock. Beyond the importance for plant growth, N availability has a strong influence on C sequestration (Fernández-Martínez et al., 2014), and hence adds another layer of urgency to why it is critical that we derive realistic representations of the total amount and dynamics of N in soil to inform current global climate research. Many terrestrial ecosystems are limited in their productivity by the availability of N for plant growth; therefore, the future response of these ecosystems to global changes as well as their ability to take up and store C may be limited by N. With estimates of biomass production increasing with climate

change (increased CO_2), N availability may hinder plant growth causing ecosystems to respond by mining for mineral-associated N in deep soil layers. Overall, this indicates that ecosystems that have deep soil and saprock stored N may be less vulnerable to changes in climate if N is plant accessible, whereas ecosystems with drier/hotter climates with less deeply stored N may be more vulnerable.

ACKNOWLEDGMENTS

Morgan Barnes was supported in part by the Institute for the Study of Ecological Effects of Climate Impacts, University of California Graduate Division, Environmental System Graduate Group, Mildred E. Mathias Graduate Research Program, and U.S. Department of Energy, Office of Biological and Environmental Research, Environmental System Science program through the River Corridor Scientific Focus Area project at the Pacific Northwest National Laboratory. The authors are grateful for the financial support from US National Science Foundation, through the Southern Sierra Critical Zone Observatory, Grant/Award Number: EAR-1331939; UC Lab Fees Research Fellowship to K. Moreland, Award Number: LGF-18-488060 from DOE-BER-TES; Lawrence Livermore National Laboratory's graduate student training fellowship to K. Moreland. A portion of the work was performed under the auspices of the US Department of Energy by Lawrence Livermore National Laboratory under Contract DE-AC52-07NA27344 (LLNL-JRNL-835846). Postdoctoral development funds from Lawrence Livermore National Laboratory also supported K Moreland (Lawrence Livermore National Laboratory is managed by UT-Battelle, LLC, for the US DOE under Contract DE-AC52-07NA27344). We would also like to thank the Stable Isotope Lab at UC Merced and the USDA Sierra National Forest. Our deepest gratitude to the reviewers and editors for their support and feedback.

DATA AVAILABILITY STATEMENT

All data are available in the manuscript itself. Datasets have been archived on Figshare. Soil nitrogen fraction data https://doi.org/10.6084/m9.figshare.19860244; Geoprobe N concentration data https://doi.org/10.6084/m9.figshare.19860313.

ORCID

Kimber C. Moreland https://orcid.org/0000-0002-5155-3348 Stephen C. Hart https://orcid.org/0000-0002-9023-6943

REFERENCES

Allison, F. E. (1973). Soil organic matter and its role in crop production. Elsevier. Amundson, R., Richter, D. D., Humphreys, G. S., Jobbágy, E. G., & Gaillardet, J. (2007). Coupling between biota and earth materials in the critical zone. *Elements*, 3(5), 327–332.

Auyeung, D. N., Martiny, J. B., & Dukes, J. S. (2015). Nitrification kinetics and ammonia-oxidizing community respond to warming and altered precipitation. *Ecosphere*, 6(5), 1–17.

Batjes, N. H. (1996). Total carbon and nitrogen in the soils of the world. *European Journal of Soil Science*, 47(2), 151–163.

Bell, C., McIntyre, N., Cox, S., Tissue, D., & Zak, J. (2008). Soil microbial responses to temporal variations of moisture and temperature in a Chihuahuan Desert grassland. *Microbial Ecology*, 56(1), 153–167.

Berhe, A. A., Harden, J. W., Torn, M. S., & Harte, J. (2008). Linking soil organic matter dynamics and erosion-induced terrestrial carbon



- sequestration at different landform positions. *Journal of Geophysical Research*: *Biogeosciences*, 113(G4). https://doi.org/10.1029/2008JG000751
- Berhe, A. A., & Torn, M. S. (2017). Erosional redistribution of topsoil controls soil nitrogen dynamics. *Biogeochemistry*, 132(1), 37–54.
- Brady, N. C., & Weil, R. R. (2016). The nature and properties of soils. Pearson Education Limited.
- Buol, S. W., McCracken, R. J., & Hole, F. D. (1980). Soil genesis and classification. Iowa State University Press.
- Chabbi, A., Kögel-Knabner, I., & Rumpel, C. (2009). Stabilised carbon in subsoil horizons is located in spatially distinct parts of the soil profile. *Soil Biology and Biochemistry*, 41(2), 256–261.
- Chapin, F. S., Matson, P. A., & Vitousek, P. M. (2011). Principles of terrestrial ecosystem ecology. Springer.
- Cleveland, C. C., Houlton, B. Z., Smith, W. K., Marklein, A. R., Reed, S. C., Parton, W., Del Grosso, S. J., & Running, S. W. (2013). Patterns of new versus recycled primary production in the terrestrial biosphere. *Proceedings* of the National Academy of Sciences, 110(31), 12733–12737.
- Conant, R. T., Ryan, M. G., Ågren, G. I., Birge, H. E., Davidson, E. A., Eliasson, P. E., Evans, S. E., Frey, S. D., Giardini, C. P., Hopkins, F. M., Hyvönen, R., Kirschbaum, M. U. F., Lavalle, J. M., Leifeld, J., & Bradford, M. A. (2011). Temperature and soil organic matter decomposition rates-synthesis of current knowledge and a way forward. Global Change Biology, 17(11), 3392–3404
- Craine, J. M., Elmore, A. J., Wang, L., Augusto, L., Baisden, W. T., Brookshire, E. J., Cramer, M. D., Hasselquist, N. J., Hobbie, E. A., Kahmen, A., Koba, K., Kranabetter, J. M., Mack, M. C., Marin-Spiotta, E., Mayor, J. R., McLauchlan, K. K., Michelsen, A., Nardoto, G. B., Oliveira, R. S., ... Zeller, B. (2015). Convergence of soil nitrogen isotopes across global climate gradients. Scientific Reports, 5(1), 1–8.
- Dahlgren, R. A., Boettinger, J. L., Huntington, G. L., & Amundson, R. G. (1997).Soil development along an elevational transect in the western Sierra Nevada, California. Geoderma, 78(3-4), 207-236.
- Dane, J. H., & Topp, C. G. (2020). Methods of soil analysis, Part 4: Physical methods (Vol. 20). John Wiley & Sons.
- Dass, P., Houlton, B. Z., Wang, Y., Wårlind, D., & Morford, S. (2021). Bedrock weathering controls on terrestrial carbon-nitrogen-climate interactions. *Global Biogeochemical Cycles*, 35(10), e2020GB006933. https://doi.org/ 10.1029/2020GB006933
- Dijkstra, P., Ishizu, A., Doucett, R., Hart, S. C., Schwartz, E., Menyailo, O. V., & Hungate, B. A. (2006). ¹³C and ¹⁵N natural abundance of the soil microbial biomass. *Soil Biology and Biochemistry*, 38(11), 3257–3266.
- Dijkstra, F. A., Morgan, J. A., Liebig, M. A., Franzluebbers, A. J., & Follett, R. F. (2012). Elevated CO₂ and warming effects on soil carbon sequestration and greenhouse gas exchange in agroecosystems: A review. In L. R. Ahuja, L. Ma (Eds.). *Methods of introducing system models into agricultural research* (pp. 467–486). ASA, CSSA, SSSA.
- Egli, M., Mirabella, A., Sartori, G., & Fitze, P. (2003). Weathering rates as a function of climate: Results from a climosequence of the Val Genova (Trentino, Italian Alps). *Geoderma*, 111(1–2), 99–121.
- Fernández-Martínez, M., Vicca, S., Janssens, I. A., Sardans, J., Luyssaert, S., Campioli, M., Chapin, F. S. III, Ciais, P., Malhi, Y., Obersteiner, M., Papale, D., Piao, S. L., Rodà, F., & Peñuelas, J. (2014). Nutrient availability as the key regulator of global forest carbon balance. *Nature Climate Change*, 4(6), 471–476.
- Follett, R. F., Stewart, C. E., Pruessner, E. G., & Kimble, J. M. (2012). Effects of climate change on soil carbon and nitrogen storage in the US Great Plains. *Journal of Soil and Water Conservation*, 67(5), 331–342.
- Gabor, R. S., Eilers, K., McKnight, D. M., Fierer, N., & Anderson, S. P. (2014). From the litter layer to the saprolite: Chemical changes in water-soluble soil organic matter and their correlation to microbial community composition. Soil Biology and Biochemistry, 68, 166–176.
- Giger, D. R., & Schmitt, G. J. (1983). Soil survey of the Sierra National Forest area, California. United States Department of Agriculture (USDA) Forest

- Service Publication, Clovis. https://www.nrcs.usda.gov/wps/portal/nrcs/surveylist/soils/survey/state/?stateId=CA
- Goulden, M. L., & Bales, R. C. (2014). Mountain runoff vulnerability to increased evapotranspiration with vegetation expansion. Proceedings of the National Academy of Sciences, 111(39), 14071–14075.
- Goulden, M. L., Anderson, R. G., Bales, R. C., Kelly, A. E., Meadows, M., & Winston, G. C. (2012). Evapotranspiration along an elevation gradient in California's Sierra Nevada. *Journal of Geophysical Research: Biogeosciences*, 117(G3). https://doi.org/10.1029/2012JG002027
- Graham, R. C., Rossi, A. M., & Hubbert, K. R. (2010). Rock to regolith conversion: Producing hospitable substrates for terrestrial ecosystems. GSA Today, 20(2), 4–9.
- Hart, S. C. (2006). Potential impacts of climate change on nitrogen transformations and greenhouse gas fluxes in forests: A soil transfer study. Global Change Biology, 12(6), 1032–1046.
- Hart, S. C., & Firestone, M. K. (1991). Forest floor-mineral soil interactions in the internal nitrogen cycle of an old-growth forest. *Biogeochemistry*, 12(2), 103–127.
- Hicks Pries, C. E., Castanha, C., Porras, R. C., & Torn, M. S. (2017). The wholesoil carbon flux in response to warming. *Science*, 355(6332), 1420– 1423.
- Hilton, R. G., Galy, A., West, A. J., Hovius, N., & Roberts, G. G. (2013). Geomorphic control on the $\delta^{15}N$ of mountain forests. *Biogeosciences*, 10(3), 1693–1705.
- Holloway, J. M., & Dahlgren, R. A. (2002). Nitrogen in rock: Occurrences and biogeochemical implications. *Global Biogeochemical Cycles*, 16(4), 65–17.
- Houlton, B. Z., & Morford, S. L. (2015). A new synthesis for terrestrial nitrogen inputs. Soil, 1(1), 381–397.
- Houlton, B. Z., Morford, S. L., & Dahlgren, R. A. (2018). Convergent evidence for widespread rock nitrogen sources in Earth's surface environment. *Science*, 360(6384), 58–62.
- Jenny, H. (1928). Relation of climatic factors to the amount of nitrogen in soils. *Agronomy Journal*, 20(9), 900–912.
- Jenny, H. (1980). The soil resource (Vol. 37). Springer.
- Jenny, H. (1994). Factors of soil formation: A system of quantitative pedology. Dover Publications.
- Jobbágy, E. G., & Jackson, R. B. (2000). The vertical distribution of soil organic carbon and its relation to climate and vegetation. *Ecological Applications*, 10(2), 423–436.
- Kaiser, K., & Guggenberger, G. (2000). The role of DOM sorption to mineral surfaces in the preservation of organic matter in soils. *Organic Geochemistry*, 31(7–8), 711–725.
- Kaiser, K., & Kalbitz, K. (2012). Cycling downwards-dissolved organic matter in soils. Soil Biology and Biochemistry, 52, 29–32.
- Kaiser, K., & Zech, W. (2000). Dissolved organic matter sorption by mineral constituents of subsoil clay fractions. *Journal of Plant Nutrition and Soil Science*, 163(5), 531–535.
- Kelly, A. E., & Goulden, M. L. (2016). A montane Mediterranean climate supports year-round photosynthesis and high forest biomass. *Tree Physiology*, 36(4), 459–468.
- Klotzbücher, T., Kaiser, K., Filley, T. R., & Kalbitz, K. (2013). Processes controlling the production of aromatic water-soluble organic matter during litter decomposition. Soil Biology and Biochemistry, 67, 133–139.
- Knicker, H. (2011). Soil organic N-An under-rated player for C sequestration in soils? Soil Biology and Biochemistry, 43(6), 1118–1129.
- Kögel-Knabner, I., Guggenberger, G., Kleber, M., Kandeler, E., Kalbitz, K., Scheu, S., Eusterhues, K., & Leinweber, P. (2008). Organo-mineral associations in temperate soils: Integrating biology, mineralogy, and organic matter chemistry. *Journal of Plant Nutrition and Soil Science*, 171(1), 61–82.
- Larsen, K. S., Andresen, L. C., Beier, C., Jonasson, S., Albert, K. R., Ambus, P., Arndal, M. F., Carter, M. S., Christensen, S., Holmstrup, M., Ibrom, A., Kongstad, J., Van der Linden, L., Maraldo, K., Michelsen, A., Mikkelsen, T. N., Pilegaard, K., Priemé, A., Ro-Poulsen, H., ... Stevnbak, K. (2011). Reduced N cycling in response to elevated CO₂, warming, and drought in



- a Danish heathland: synthesizing results of the CLIMAITE project after two years of treatments. *Global Change Biology*, *17*(5), 1884–1899.
- LeBauer, D. S., & Treseder, K. K. (2008). Nitrogen limitation of net primary productivity in terrestrial ecosystems is globally distributed. *Ecology*, 89(2), 371–379.
- Lybrand, R. A., Heckman, K., & Rasmussen, C. (2017). Soil organic carbon partitioning and Δ^{14} C variation in desert and conifer ecosystems of southern Arizona. *Biogeochemistry*, 134(3), 261–277.
- Manzoni, S., Schimel, J. P., & Porporato, A. (2012). Responses of soil microbial communities to water stress: results from a meta-analysis. *Ecology*, 93(4), 930–938.
- McFarlane, K. J., Torn, M. S., Hanson, P. J., Porras, R. C., Swanston, C. W., Callaham, M. A., & Guilderson, T. P. (2013). Comparison of soil organic matter dynamics at five temperate deciduous forests with physical fractionation and radiocarbon measurements. *Biogeochemistry*, 112(1), 457–476
- McGill, W. B., & Cole, C. V. (1981). Comparative aspects of cycling of organic C, N, S and P through soil organic matter. *Geoderma*, 26(4), 267–286.
- Mikutta, R., Turner, S., Schippers, A., Gentsch, N., Meyer-Stüve, S., Condron, L. M., Peltzer, D. A., Richardson, S. J., Eger, A., Hempel, G., Kaiser, K., Klotzbücher, T., & Guggenberger, G. (2019). Microbial and abiotic controls on mineral-associated organic matter in soil profiles along an ecosystem gradient. Scientific Reports, 9(1), 1–9.
- Moreland, K. (2020). Climatic controls on deep soil carbon and nitrogen dynamics. [Doctoral dissertation], University of California, Merced. ProQuest Dissertations Publishing Accession No. 10585.
- Moreland, K., Tian, Z., Berhe, A. A., McFarlane, K. J., Hartsough, P., Hart, S. C., Bales, R., & O'Geen, A. T. (2021). Deep in the Sierra Nevada critical zone: Saprock represents a large terrestrial organic carbon stock. Environmental Research Letters, 16(12), 124059. https://doi.org/10.1088/1748-9326/ac3bfe
- Niboyet, A., Le Roux, X., Dijkstra, P., Hungate, B. A., Barthes, L., Blankinship, J. C., Brown, J. R., Field, C. B., & Leadley, P. W. (2011). Testing interactive effects of global environmental changes on soil nitrogen cycling. *Ecosphere*, 2(5), 1–24.
- O'Geen, A., Safeeq, M., Wagenbrenner, J., Stacy, E., Hartsough, P., Devine, S., Tian, Z., Ferrell, R., Goulden, M., Hopmans, J. W., & Bales, R. (2018). Southern Sierra Critical Zone Observatory and Kings River Experimental Watersheds: A synthesis of measurements, new insights, and future directions. *Vadose Zone Journal*, 17(1), 1–18.
- Pope, G. A. (1995). Internal weathering in quartz grains. *Physical Geography*, 16(4), 315–338.
- Rasmussen, C., Southard, R. J., & Horwath, W. R. (2007). Soil mineralogy affects conifer forest soil carbon source utilization and microbial priming. Soil Science Society of America Journal, 71(4), 1141–1150.
- Rasmussen, C., Torn, M. S., & Southard, R. J. (2005). Mineral assemblage and aggregates control carbon dynamics in a California conifer forest. Soil Science Society of America Journal, 69(6), 1711–1721.
- Riebe, C. S., Hahm, W. J., & Brantley, S. L. (2017). Controls on deep critical zone architecture: A historical review and four testable hypotheses. *Earth Surface Processes and Landforms*, 42(1), 128–156.
- Ros, G. H., Hoffland, E., Van Kessel, C., & Temminghoff, E. J. (2009). Extractable and dissolved soil organic nitrogen—A quantitative assessment. Soil Biology and Biochemistry, 41(6), 1029–1039.
- Rumpel, C., & Kögel-Knabner, I. (2011). Deep soil organic matter—A key but poorly understood component of terrestrial C cycle. *Plant and soil*, 338(1), 143–158.
- Rustad, L. E. J. L., Campbell, J., Marion, G., Norby, R., Mitchell, M., Hartley, A., Cornelissen, J., & Gurevitch, J. (2001). A meta-analysis of the response of soil respiration, net nitrogen mineralization, and aboveground plant growth to experimental ecosystem warming. *Oecologia*, 126(4), 543– 562.
- Schrumpf, M., & Kaiser, K. (2015). Large differences in estimates of soil organic carbon turnover in density fractions by using single and repeated radiocarbon inventories. *Geoderma*, 239, 168–178.

- Schrumpf, M., Kaiser, K., Guggenberger, G., Persson, T., Kögel-Knabner, I., & Schulze, E. D. (2013). Storage and stability of organic carbon in soils as related to depth, occlusion within aggregates, and attachment to minerals. *Biogeosciences*, 10(3), 1675–1691.
- Shangguan, W., Hengl, T., Mendes de Jesus, J., Yuan, H., & Dai, Y. (2017). Mapping the global depth to bedrock for land surface modeling. *Journal of Advances in Modeling Earth Systems*, 9(1), 65–88.
- Sistla, S. A., & Schimel, J. P. (2012). Stoichiometric flexibility as a regulator of carbon and nutrient cycling in terrestrial ecosystems under change. New Phytologist, 196(1), 68–78.
- Sleutel, S., Vandenbruwane, J., De Schrijver, A., Wuyts, K., Moeskops, B., Verheyen, K., & De Neve, S. (2009). Patterns of dissolved organic carbon and nitrogen fluxes in deciduous and coniferous forests under historic high nitrogen deposition. *Biogeosciences*, 6(12), 2743–2758.
- Stevenson, F. J. (1962). Chemical state of the nitrogen in rocks. *Geochimica et Cosmochimica Acta*, 26(7), 797–809.
- Stuiver, M., & Polach, H. A. (1977). Discussion reporting of 14C data. *Radiocarbon*, 19(3), 355–363.
- Swanston, C. W., Caldwell, B. A., Homann, P. S., Ganio, L., & Sollins, P. (2002). Carbon dynamics during a long-term incubation of separate and recombined density fractions from seven forest soils. Soil Biology and Biochemistry, 34(8), 1121–1130.
- Tian, Z., Hartsough, P. C., & O'Geen, A. T. (2019). Lithologic, climatic and depth controls on critical zone transformations. Soil Science Society of America Journal, 83(2), 437–447.
- Thomas, G. W. (1996). Soil pH and soil acidity. In D. L. Sparks, A. L. Page, P. A. Helmke, & R. H. Loeppert (Eds.), *Methods of soil analysis*, Part 3 (pp. 475–490). SSSA.
- Tonneijck, F. H., & Jongmans, A. G. (2008). The influence of bioturbation on the vertical distribution of soil organic matter in volcanic ash soils: A case study in northern Ecuador. *European Journal of Soil Science*, *59*(6), 1063– 1075.
- Trumbore, S. E., & Harden, J. W. (1997). Accumulation and turnover of carbon in organic and mineral soils of the BOREAS northern study area. *Journal of Geophysical Research*: Atmospheres, 102(D24), 28817–28830.
- US Department of Agriculture. (2019). Keys to soil taxonomy. USDA.
- Uselman, S. M., Qualls, R. G., & Lilienfein, J. (2012). Quality of soluble organic C, N, and P produced by different types and species of litter: Root litter versus leaf litter. *Soil Biology and Biochemistry*, *54*, 57–67.
- Van Groenigen, J. W., Huygens, D., Boeckx, P., Kuyper, T. W., Lubbers, I. M., Rütting, T., & Groffman, P. M. (2015). The soil N cycle: New insights and key challenges. Soil, 1(1), 235–256.
- Vitousek, P. M., & Howarth, R. W. (1991). Nitrogen limitation on land and in the sea: How can it occur? *Biogeochemistry*, 13(2), 87–115.
- Vogel, J. S., Southon, J. R., Nelson, D. E., & Brown, T. A. (1984). Performance of catalytically condensed carbon for use in accelerator mass spectrometry. Nuclear Instruments and Methods in Physics Research Section B: Beam Interactions with Materials and Atoms, 5(2), 289–293.
- von Lützow, M., Kögel-Knabner, I., Ekschmitt, K., Matzner, E., Guggenberger, G., Marschner, B., & Flessa, H. (2006). Stabilization of organic matter in temperate soils: Mechanisms and their relevance under different soil conditions—a review. *European Journal of Soil Science*, 57(4), 426–445.
- Wang, C., Chen, Z., Unteregelsbacher, S., Lu, H., Gschwendtner, S., Gasche, R., Kolar, A., Schloter, M., Kiese, R., Butterbach-Bahl, K., & Dannenmann, M. (2016). Climate change amplifies gross nitrogen turnover in montane grasslands of Central Europe in both summer and winter seasons. Global Change Biology, 22(9), 2963–2978.
- Wieder, W. R., Cleveland, C. C., Smith, W. K., & Todd-Brown, K. (2015). Future productivity and carbon storage limited by terrestrial nutrient availability. *Nature Geoscience*, 8(6), 441–444.
- Yang, Y., Berhe, A. A., Barnes, M. E., Moreland, K. C., Tian, Z., Kelly, A. E., Bales, R. C., O'Geen, A. T., Goulden, M. L., Hartsough, P., & Hart, S. C. (2022). Climate warming alters nutrient storage in seasonally

dry forests: Insights from a 2300 m elevation gradient. *Global Biogeochemical Cycles*, 36(11), e2022GB007429. https://doi.org/10.1029/2022GB007429

Yost, J. L., & Hartemink, A. E. (2020). How deep is the soil studied-An analysis of four soil science journals. *Plant and soil*, 452(1), 5–18.

Young, J. L., & Spycher, G. (1979). Water-dispersible soil organic-mineral particles: I. Carbon and nitrogen distribution. Soil Science Society of America Journal, 43(2), 324–328. How to cite this article: Moreland, K. C., Barnes, M. E., O'Geen, A., Dove, N., Hart, S. C., & Berhe, A. A. (2023). Climatic controls on soil and saprock nitrogen distribution and persistence in the Sierra Nevada. *Journal of Plant Nutrition and Soil Science*, 186, 116–129. https://doi.org/10.1002/jpln.202200218